

Supplementary Information

Novel Au-anchored Fe-NC nanozyme enabled rapid and sensitive colorimetric detection of Cr(VI)

Shumin Xi,^{†a,c} Fengjun Luo,^{†b} Peng Chen,^a Ding Wang,^{*a} Jingxi Wang,^{*b} Beibei

Kou,^{*d} Renyong Zhao^c

a School of Chemistry and Chemical Engineering, Chongqing University of Technology, Chongqing, 400054, PR China;

b Chongqing Key Laboratory of New Energy Storage Materials and Devices, College of Physics and New Energy, Chongqing University of Technology, Chongqing, 401135, PR China;

c School of Food Science and Technology, Henan University of Technology, Zhengzhou, Henan, 450001, PR China;

d State Key Laboratory of High-efficiency Utilization of Coal and Green Chemical Engineering, School of Chemistry and Chemical Engineering, Ningxia University, Yinchuan, Ningxia, 750021, PR China.

CONTENTS

Stability of AuNPs/Fe-NC during the catalytic process	S-3
Circulation and storage stability of AuNPs/Fe-NC nanozyme	S-4
Table S1 Comparison of steady-state kinetic parameters of AuNPs/Fe-NC nanozyme with another report peroxidase mimics	S-5
Verification the generation of $\cdot\text{OH}$ during the H_2O_2 catalysis by AuNPs/Fe-NC	S-6
Optimization of the Cr(VI) detection conditions	S-7
Anti-interference analysis for colorimetric detection of Cr(VI)	S-8
References	S-9

Stability of AuNPs/Fe-NC during the catalytic process

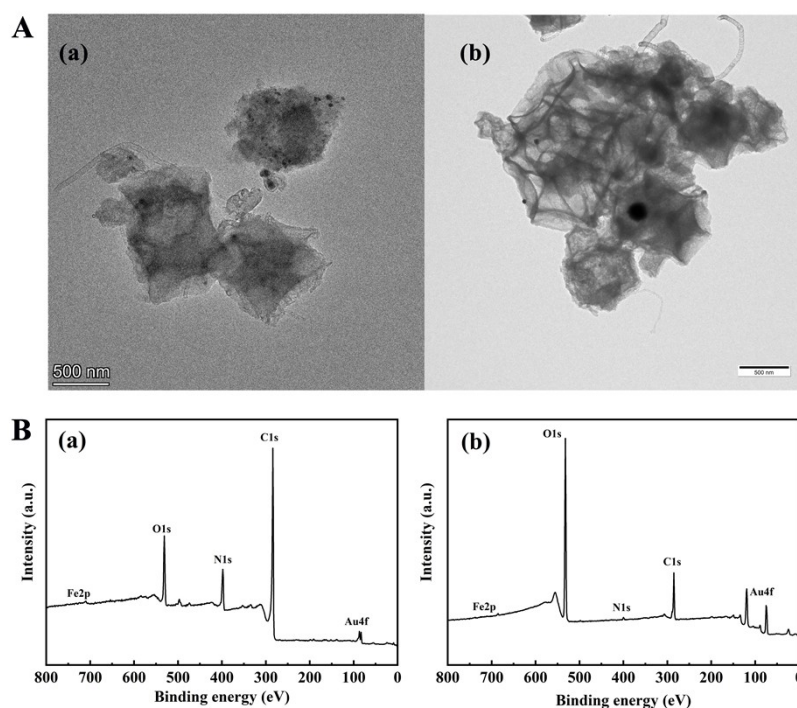


Figure S1 (A) TEM and (B) XPS characterizations of AuNPs/Fe-NC (a) before and (b) after the catalytic reaction.

It is a very valuable research to explore the stability of AuNPs/Fe-NC nanozyme during the detection process. In this work, a comparison of the morphology and composition of the prepared AuNPs/Fe-NC before and after the catalytic reaction was conducted by TEM and XPS analysis. As shown in Figure S1A, no significant change in the morphology of the material before and after the catalytic reaction. Meanwhile, XPS comparative analysis also confirmed that the material has good stability (seen in Figure S1B). From the above results, we could conclude the stability of prepared nanozyme, which also could be attributed to the relatively mild catalytic reaction environment.

Circulation and storage stability of AuNPs/Fe-NC nanozyme

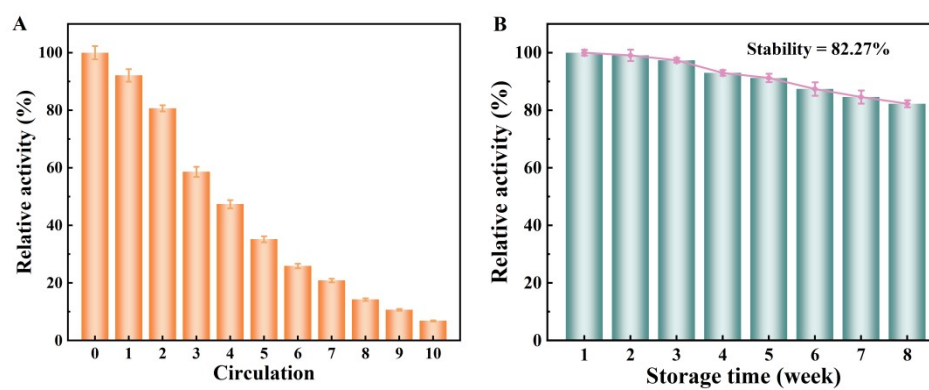


Figure S2 Stability analysis of AuNPs/Fe-NC nanozyme.

Table S1 Comparison of steady-state kinetic parameters of AuNPs/Fe-NC nanozyme with another report peroxidase mimics.

Catalyst	K_m / (mM)		V_{max} / (10^{-7} M/s)		Reference
	TMB	H ₂ O ₂	TMB	H ₂ O ₂	
Au seeds	0.088	47.56	0.17	0.178	[1]
Fe ₃ O ₄	0.233	479.91	17.66	27.5	[2]
Fe ₃ O ₄ @MQDs	0.36	6.81	2.89	24	[3]
Fe ₃ O ₄ @MoS ₂	0.25	1.39	11.1	16.3	[4]
PtPd NPs	1.78	0.053	3.64	0.926	[5]
Pd@Pt	0.067	490	1.2	1.2	[6]
Fe ₃ O ₄ @C ₇	0.057	0.863	0.62	0.856	[7]
AuNPs/Fe-NC	0.433	1.299	11.976	2.305	This work

Verification the generation of $\cdot\text{OH}$ during the H_2O_2 catalysis by AuNPs/Fe-NC

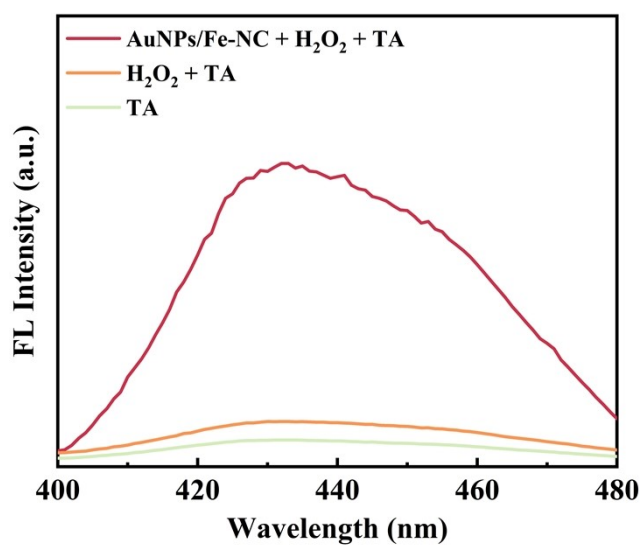


Figure S3 Fluorescent curves of TA, H_2O_2 + TA, and AuNPs/Fe-NC + H_2O_2 + TA.

Fluorescence analysis method was further applied to demonstrate the generation of $\cdot\text{OH}$. Terephthalic acid (TA) as a typically fluorescent probe can capture hydroxyl radical ($\cdot\text{OH}$) to produce a fluorescent product with an emission at 440 nm. As expected, only if the AuNPs/Fe-NC, H_2O_2 , and TA are all existed, an obvious fluorescent signal was observed, demonstrating the generation of $\cdot\text{OH}$ during the catalytic reaction.

Optimization of the Cr(VI) detection conditions

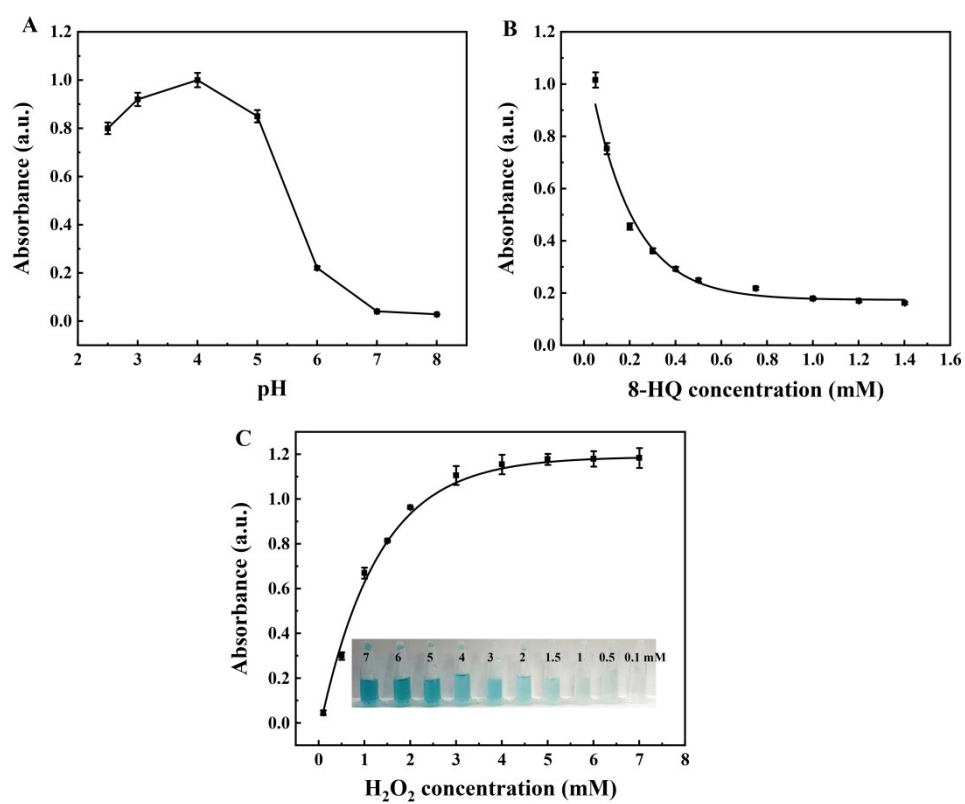


Figure S4 Optimization of the Cr(VI) detection conditions (A) pH; (B) 8-HQ concentration, and (C) H₂O₂ concentration

Anti-interference analysis for colorimetric detection of Cr(VI)

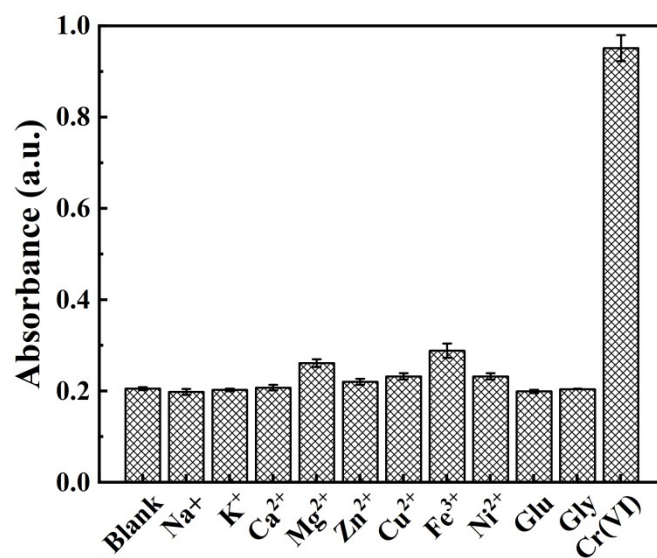


Figure S5 Anti-interference analysis for colorimetric detection of Cr(VI)

References

- [1] C.X. Guo, D.H. Liu, W.B. Xu, et al. Accelerating the peroxidase and glucose oxidaselike activity of Au nanoparticles by seeded growth strategy and their applications for colorimetric detection of dopamine and glucose. *Colloids and Surfaces A: Physicochemical and Engineering Aspects*, **2022**, 658, 130555.
- [2] L.Z. Gao, J. Zhuang, L. Nie, et al. Intrinsic peroxidase-like activity of ferromagnetic nanoparticles. *Nature Nanotechnology*, **2007**, 2, 577-583.
- [3] Y.H. Cheng, P. Shen, X.C. Li, et al. Synergistically enhanced peroxidase-like activity of Fe₃O₄/Ti₃C₂ MXene quantum dots and its application in colorimetric determination of Cr (VI). *Sensors and Actuators B: Chemical*, **2023**, 376, 132979.
- [4] F. Wei, X.Y. Cui, Z. Wang, et al. Recoverable peroxidase-like Fe₃O₄@MoS₂-Ag nanozyme with enhanced antibacterial ability. *Chemical Engineering Journal*, **2021**, 408, 127240.
- [5] T. Jiang, Y. Song, D. Du, et al. Detection of p53 protein based on mesoporous Pt-Pd nanoparticles with enhanced peroxidase-like catalysis. *ACS Sensors*, **2016**, 1, 717-724.
- [6] W.G. Wang, R.K. Du, C.Z. Dong, et al. A modified sensitive ELISA based on dual catalysis of Pd@Pt porous nanoparticles and horseradish peroxidase. *Sensors and Actuators B: Chemical*, **2019**, 284, 475-484.
- [7] J.Q. Wen, Z. Yun, Z.L. Cheng, et al. Peroxidase-like activity of Fe₃O₄@fatty acidnanoparticles and their application for the detection of uric acid. *New Journal of Chemistry*, **2020**, 44, 18608-18615.